

## Lattice-soliton scattering in nonlinear atomic chains

Qiming Li,\* St. Pnevmatikos, E. N. Economou, and C. M. Soukoulis\*

*Research Center of Crete, and Department of Physics,  
University of Crete, 71110 Heraklio, Crete, Greece*

(Received 11 June 1987; revised manuscript received 21 September 1987)

We have studied numerically the soliton scattering from one or two impurities in one-dimensional atomic lattices with nonlinear first-neighbor interactions of both quartic and Morse type. Our results for small-amplitude incident solitons are interpreted with some analytical formulas obtained from linear theories, while comparison with linear wave-packet results are made for both low- and high-amplitude incident solitons. Finally, interference effects are studied.

### I. INTRODUCTION

During the last 30 years, there has been a great deal of interest among solid-state physicists in the problem of wave propagation in harmonic crystals with impurities. More recently, scientists were oriented to the study of nonlinearity in atomic systems and especially to soliton propagation in homogeneous anharmonic chains. This paper is the first step in our effort to understand the combined effects of disorder and nonlinearity, and particularly, to clarify whether or not nonlinearity modifies qualitatively the effects of disorder on transport properties. Here we are studying soliton scattering on one or two impurities in one-dimensional atomic lattices with nonlinear first-neighbor interactions.

Another complementary way of studying the effects of nonlinearity in disordered systems is by using the disordered tight-binding Hamiltonian with an extra nonlinear term. The scattering of a plane wave from the disordered part with nonlinearity is studied.

Nonlinearity can approximately mimic some direct or phonon-mediated electron-electron interactions. Thus these studies may be very useful in expanding our understanding of disorder and interactions in solids.

The classical example of such a system is the Fermi-Pasta-Ulam (FPU) chain<sup>1</sup> where particles are coupled with harmonic plus cubic (or quartic) nonlinear first-neighbor interactions. The continuum limit of this model, for different orders, is either a Boussinesq type<sup>2</sup> or a nonlinear Schrödinger (NLS) equation<sup>3</sup> which admit non-topological soliton solutions, e.g., collective, localized in space excitations which for the FPU chains are simple compressions or rarefactions with the convenient soliton shape. These excitations propagate in the pure system without losing their integrity or changing their velocity, even after several interactions with other solitons.

Propagation of a kink (pulse) soliton in nonlinear lattices with an impurity has been studied not only theoretically and numerically, but also experimentally using nonlinear electric transmission lines.<sup>4,5</sup> This problem is related to stability of the soliton in disordered lattices and also to thermal conductivity in disordered anharmonic systems.<sup>6,7</sup> However, these results are limited either to the idealized Toda lattice,<sup>8</sup> or if extended to more common

anharmonic chains,<sup>9,10</sup> are valid only for small-amplitude pulse-type solitons. In all these cases, one uses the inverse scattering method to treat the homogeneous part of the chain and assumes a linear behavior during the soliton-impurity scattering to correct the results using perturbation techniques. The nonlinearity here, while necessary to ensure the balance of the dispersion and the stability of the soliton, is not enough to change the usual scattering properties of the wave packets.

In our numerical study we examine the complete range of soliton energies including both small- and large-amplitude pulse solitons using as initial conditions for the last case numerical solutions for narrow solitons obtained recently.<sup>11</sup> In addition we study the very important class of envelope solitons, and we relate our results for the linear energy excitations with some formulas from the linear theory.<sup>12</sup> Finally, we discuss some interference effects from two impurity scatterings for both pulse and envelope soliton excitations.

Our model and a brief review of the lattice soliton solutions are presented in Sec. II. In Sec. III we discuss our results, and finally in Sec. IV we present our conclusions.

### II. FORMALISM AND NUMERICAL PROCEDURES

We consider a monoatomic chain of first-neighbor interacting particles with the Hamiltonian

$$H = \sum_n \left[ \frac{1}{2} M_n \dot{y}_n^2 + V(y_n - y_{n-1}) \right], \quad (2.1)$$

where  $y_n(t)$  denotes the longitudinal displacement of the  $n$ th atom from its equilibrium position  $\dot{y}_n = dy_n/dt$  and  $M_n = \gamma M$  ( $\gamma \neq 1$  only for  $n = n_0$ , where  $n_0$  is the impurity site). The interaction potential  $V(r_n)$ , where  $r_n = y_n - y_{n-1}$  is the bond strain, can be quite general, but in this paper we limit our attention to the two following forms:

$$(i) \text{ cubic and quartic: } V(r) = Gr^2/2 + Ar^3/3 + Br^4/4, \quad (2.2)$$

$$(ii) \text{ Morse: } V(r) = P(e^{-ar} - 1)^2. \quad (2.3)$$

In both cases above, the parameters in the interaction potentials can be determined to fit each other for small  $r$

( $r \ll D$ , where  $D$  is the lattice spacing). The equation of motion for  $y_n$  can be written as

$$M_n \ddot{y}_n = -V'(y_n - y_{n-1}) + V'(y_{n+1} - y_n), \quad (2.4)$$

where  $V'(r) = dV/dr$ . For simplicity, we take  $M = D = t = 1$ .

One can obtain approximate solutions of Eq. (2.4) in the continuum limit, using well-known techniques.<sup>2,3</sup> In this limit, one can expand the Morse potential (and any other empirical pair potential) to obtain the polynomial form of Eq. (2.2) and retain just the first and/or the second nonlinear term. For the exact Morse form, no analytical solutions exist. Then, for slowly varying solitary waves of the form  $y(x - vt)$ , where  $v$  is the group velocity ( $v = \text{const.}$ ), one can obtain either a Boussinesq type or a NLS equation with different soliton solutions.

Thus looking for kink soliton solutions (pulse for the relative displacement) and using an improved quasicon- tinuum approximation,<sup>13</sup> we transform Eq. (2.4) with the potential (2.2) for the homogeneous system to a general- ized Boussinesq ( $G - Bq$ ) equation<sup>2</sup> with the velocity- dependent dispersion coefficient:

$$u_{tt} - c_0^2 u_{xx} - p(u^2)_{xx} - q(u^3)_{xx} - hu_{xxxx} = 0, \quad (2.5)$$

where  $c_0^2 = GD^2/M$ ,  $h = GD^4v^2/(12Mc_0^2)$

$$u = y_x, \quad p = AD^3/M, \quad q = BD^4/M. \quad (2.6)$$

The analytical solutions of Eq. (2.5) are summarized in Appendix A. Here we discuss their general properties. For  $B$  (or  $q$ )  $< 0$  (inverted quartic potential), there are no solitary excitations. For  $B > 0$  and  $A \neq 0$ , there are both compressive and rarefactive kinks, but in the continuum limit only the one that has the same sign as  $A$  (or  $p$ ) is stable. For  $B > 0$  and  $A = 0$  (quartic potential) both compressive and rarefactive kinks exist and are stable. Since the empirical pair potentials (e.g., Morse, etc.) have  $A < 0$  when expanded near the equilibrium position, the kinks are compressive and feel the repulsive part of the potential. (For a detailed account of these properties for kink solitons see Ref. 14.) In our case, since  $h > 0$ , we always have supersonic kink solitons with  $v > c_0$ , where the velocity  $v$  is the only free parameter of the solution. Even in this improved quasicon- tinuum approximation, the known analytic solutions (see Appendix A) break down when the width of the excitations is comparable to the lattice spacing  $D$  (e.g., when  $v \gg c_0$ ). However, for the monoatomic chain, we have found numerically stable narrow kinks which propagate without radiation even with very high velocities where the amplitude of the rare- faction (or compression) becomes comparable to the lat- tice spacing ( $r_{\text{max}} \sim D$ ).<sup>11</sup> In the other limit, when  $v \rightarrow c_0$  the amplitude of the wave tends to zero while the width tends to infinity so that the wave disappears. However, while the nonlinear terms in the potential are very small and the wave behaves like linear excitation, they are necessary to balance dispersion and ensure the long life- time of the soliton.

Looking for oscillating localized solutions of the form

$$\begin{aligned} y_n(t) &= \sum_j \epsilon^j \psi_j(n, t) \\ &= \sum_j \epsilon^j \sum_m F_{jm}(n, t) e^{im\theta} + \text{c.c.}, \end{aligned} \quad (2.7)$$

with  $\theta = knD - \omega t$  and where  $\epsilon$  is a small scaling param- eter, we can treat the phase  $\theta(n, t)$  exactly and only use the continuum approximation for the envelope function  $F(x, t)$ . For the quartic potential we have seen<sup>3</sup> that only the terms for  $j = 1$  and  $m = 1$  contribute and the relation (2.7) reduces to the simplest formula

$$y_n(t) = \epsilon F_{11}(n, t) e^{i\theta} + \text{c.c.} \quad (2.8)$$

The amplitude  $F_{11}(n, t)$  in the continuum limit [retaining terms up to the order  $O(\epsilon^3)$ ] satisfies the following NLS equation:

$$iF_\tau + \frac{1}{2}F_{\xi\xi} + \kappa_O |F|^2 F = 0, \quad (2.9)$$

where  $F(x, t) = F_{11}(n, t)$  is a complex function with a smoothly oscillating part  $\xi = x - v_g t$  and  $\tau = \mu t$ , with  $v_g = d\omega/dk$ ,  $\mu = d^2\omega/dk^2$ , and the frequency  $\omega$  is given as a function of the wave vector  $k$  by the linear dispersion relation:

$$\omega^2 = 4 \frac{G}{M} \sin^2(kD/2). \quad (2.10)$$

Finally,  $\kappa_O = Q/\mu$ , where

$$Q = - \frac{24}{\omega} \frac{B}{M} \sin^4(kD/2). \quad (2.11)$$

When  $\kappa_O > 0$ , Eq. (2.9) allows a pulse-type envelope soli- ton solution which with formula (2.8) defines the oscillat- ing soliton form for the discrete lattice. When  $\kappa_O < 0$ , Eq. (2.9) allows dark-type excitons.<sup>2</sup> For the cubic po- tential or the cubic quartic, however, in deriving the cor- responding NLS equation one must keep consistently higher orders in  $\epsilon$  and higher harmonics, even though a few of them are sufficient.<sup>3</sup>

The analytic solution of Eq. (2.9) combined with Eq. (2.8) for the envelope-type soliton is given in Appendix B. Here we summarize its general properties. While the car- rier wave of the envelope soliton follows to the order  $\epsilon$  (the same dispersion relation with the plane wave in the harmonic limit) the excitation remains localized (solitary) due to the pulse-type modulating part which balances the dispersive tendency and gives the soliton a long lifetime. The soliton frequency  $\Omega = \omega - 2\alpha v_g + 2\mu(\alpha - \eta)$  and wave vector  $K = k - 2\alpha$  include only small nonlinear correc- tions compared to the harmonic values  $\omega$  and  $k$ , because  $\alpha$  and  $\eta$  are small to order  $O(\epsilon)$  parameters. Thus the soliton velocity  $v_e$  follows to the order  $\epsilon$  the linear group velocity  $v_g$  and remains always subsonic ( $v_e \leq c_0$ ). The quantities  $\alpha$  and  $\eta$  together with the wave vector  $k$  are the free parameters of the solution but only  $k$  exhibits a large range of values, i.e., the whole of the first Brillouin zone. The amplitude  $A_m$  and the width  $L_e$  depend on the parameter  $\eta$  so that when  $A_m \rightarrow 0$ ,  $L_e \rightarrow \infty$ , and the envelope soliton disappears. However, in order to preserve the balance between dispersion and nonlinearity, one must consider consistently the parameters when

$\eta \gg O(\epsilon)$ ; in this case analytic solutions break down, the excitation becomes very narrow, and propagates with permanent radiation losing its soliton properties.

In a series of previous publications<sup>2,3,11,14</sup> it has been confirmed that our homogeneous system supports stable propagation of these soliton solutions. Here, we consider the same chain but with a mass impurity to occupy the site  $n_0$ . Due to the soliton-impurity interaction, the incident wave is decomposed to a transmitted plus a reflected part, while in some cases the impurity may be excited and a localized or a resonant mode may appear. Even after this decomposition of the incident soliton, we can recognize one or more solitons of the same type appearing asymptotically in the transmitted and/or in the reflected part accompanied by some small amplitude oscillations. In Fig. 1, we show qualitatively such a scattering process for both a pulse and an envelope soliton propagating in a chain with quartic interactions. The impurity  $M_0 = 0.1M$  is sited in cell 128. Due to both the small mass size of the impurity and the small amplitude of the incident soliton, the transmitted wave is soon adapted to a new single soliton while the reflected waves are decomposed to ripples.

Except for some particular cases,<sup>8-10</sup> one has no

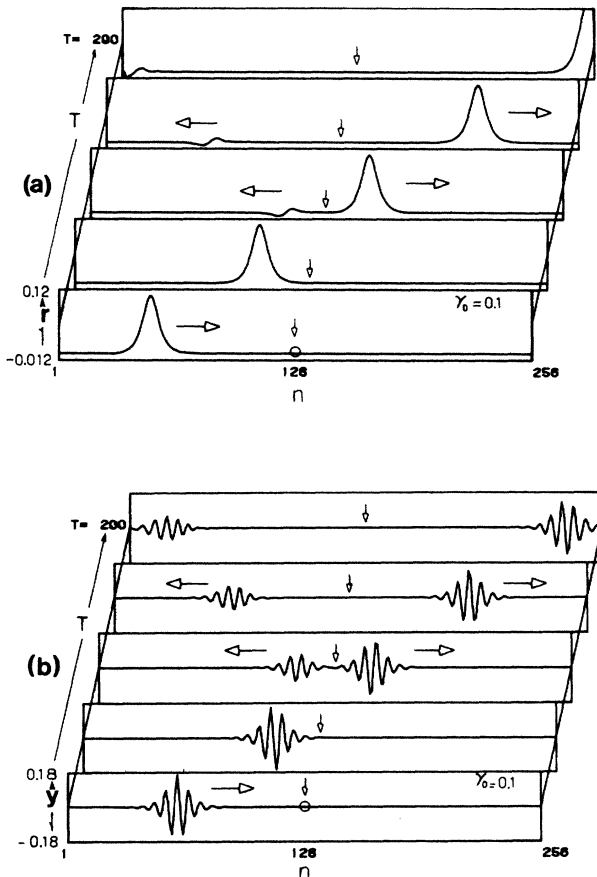


FIG. 1. Soliton impurity scattering in a quartic potential chain ( $G=B=1$ ) with  $\gamma=0.1$  for different times  $T$ . (a) Pulse incident soliton (for relative displacement representation). (b) Envelope incident soliton (for absolute displacement representation).

analytical theory to treat the nonlinear wave scattering on a single impurity, thus we study here this problem numerically. With a fourth-order Runge-Kutta method, we integrate the set of Eq. (2.4), including one equation for the impurity mass. Our simulations begin with initial conditions coinciding with one of the analytical or numerical solutions described previously. In our model, which is a conservative one, in order to check the accuracy of the integration we follow the numerical error for the total energy which in all cases is less than  $10^{-2}\%$ .

On the other hand, much analytical and numerical work has been done on one-dimensional (1D) disordered systems.<sup>12,15</sup> It is well known that all the eigenstates in 1D disordered systems are exponentially localized. The rate of the exponential decay defines the localization length<sup>12</sup> which is proportional to  $W^{-2}$ , where  $W$  is the strength of the disorder. The role of the nonlinearity on disordered systems has only recently begun to be studied.<sup>16</sup> It will be of considerable interest to see how the exponentially localized states of the disordered systems will behave in the presence of the nonlinearity. Our way of calculating the effects of the nonlinearity in disordered systems can be viewed as complementary to that of Souillard.<sup>16</sup> Here we have a nonlinear medium, where the soliton is a solution, and see how this soliton behaves in the presence of impurities. Souillard has studied a linear tight-binding model with no disorder in which an incoming segment exhibiting both disorder and nonlinearity is embedded; the question is how a plane wave propagates through this segment.

### III. RESULTS AND DISCUSSION

In this section we compute the soliton transmission coefficient which may be defined in three different ways: (i) the total transmitted energy including the energy of all the transmitted solitons plus the radiative part over the soliton incident energy  $T = E_t/E_i$ ; (ii) the total soliton transmitted energy which includes only the energy of all the transmitted solitons which may be more than one over the incident soliton energy  $T_s = E_s/E_i$ ; (iii) the energy of the first transmitted soliton over the incident soliton energy  $T_1 = E_1/E_i$ . We can define the reflection coefficient in a similar way.

#### A. Weak nonlinear case (low-energy solitons)

In this case we study small-amplitude kink (or pulse) soliton as well as envelope solitons. For these waves the nonlinear terms in Eq. (2.2) are small compared to the harmonic term. Hence, the process of scattering can be treated in three steps: (a) traveling of the incoming soliton in the homogeneous nonlinear lattice before scattering, (b) linear scattering of the solitary wave, and (c) traveling of the transmitted and reflected wave in the homogeneous nonlinear lattice after scattering. The linear scattering of the soliton shape wave packet can be solved exactly by Fourier transforming. In this context, the transmission coefficient for linear wave packets (LWP) is given by

$$T_{\text{LWP}} = \frac{\int_{-\pi}^{\pi} dk |a(k)|^2 |t(k)|^2 \sin^2(kD/2)}{\int_{-\pi}^{\pi} dk |a(k)|^2 \sin^2(kD/2)}, \quad (3.1)$$

where

$$a(k) = \sum_{n=-\infty}^{\infty} y_n(0) e^{iknD} \quad (3.2)$$

is the Fourier component of the incident soliton and  $t(k)$  is the transmission amplitude of the linear plane wave (LPW) with wave vector  $k$ . To obtain Eq. (3.1), we have assumed that outgoing Fourier components of the incident soliton can be neglected. This is the case for low-energy solitons where  $V_s \sim c$  and  $w(k) \simeq ck$ . Using an analogy between the tight-binding electron scattering problem and the lattice wave scattering problem,<sup>12</sup> we can easily obtain the transmission amplitude of a linear plane wave scattered by one mass impurity.

$$M_0 = \gamma M, \quad (3.3)$$

$$t(k) = \frac{2i \sin kD}{2i \sin kD + 2(\gamma - 1)(1 - \cos kD)}$$

and the transmission coefficient:

$$T_{\text{LPW}}(k) = |t(k)|^2 = \frac{1}{1 + (\gamma - 1)^2 \tan^2(kD/2)}. \quad (3.4)$$

In the case of weak scattering, the transmitted soliton almost takes all the transmitted energy. So we can assume  $T = T_s = T_{\text{LWP}}$ . We will also make a further approximation  $T_{\text{LWP}} \simeq T_{\text{LPW}}(K_s)$ , where  $K_s$  is one appropriately defined soliton wave vector. For kink solitons in the continuum limit, one can use, as a first-order approximation, the  $K_s = 1/L$  given in Appendix A for the cubic (first nonlinear approximation of the Morse) and quartic potential cases. While for envelope solitons, we use as  $k$  the  $K_s = 1/L_0 = k - 2a$  (see Appendix B). As we can see in the following discussion, this approximation gives a very good account for the weak-scattering behavior. For convenience, we introduce the new coefficient

$$S \equiv \frac{1}{T_s} - 1 \simeq (\gamma - 1)^2 \tan^2 K_s D / 2, \quad (3.5)$$

where for small  $K_s$  (continuum limit)  $S = (\gamma - 1)^2 (K_s D)^2 / 4$ . In Fig. 2, we plot  $S$  as a function of  $(\gamma - 1)^2$  to show the mass dependence of the transmission coefficient for three different soliton energies. These results prove the linear scattering behavior for small energies and the small mass ratio predicted by the analytic formula (3.5). When the soliton energy is higher, the deviation becomes larger (especially for high mass ratio).

In order to present the dependence of  $S$  on incident soliton energy, one can use again the formula (3.5) expressing  $K_s$  through the incident energy  $E_i$ . This can be done in the continuum limit by using the energy formulas of Appendix A. Assuming that  $v^2 \simeq c_0^2$  and  $K_s \ll 1$ , we obtain  $S \sim E_i^{2/3}$  for the cubic (first nonlinear approximation of the Morse) which is consistent with the results of Yoshida and Sakuma.<sup>9</sup>

For the quartic potential, we obtain  $S \sim E_i^2$ . In Fig. 3

we show this dependence of  $S$  on incident soliton energy for the quartic and Morse potential chain.

The  $E^2$  dependence for quartic and  $E^{2/3}$  for Morse potential is followed at the low-energy regime. Again, when impurity mass and energy get larger, deviations become larger. The deviations come from two sources. One source is the use of a single value  $K_s$  instead of full Fourier transform. When impurity mass gets larger,  $T(K_s)$  falls fast for larger values of  $K_s$ ; therefore, contributions from  $K < K_s$  may be important. For a narrow soliton,  $\Delta k$  is large, therefore, a single wave vector plane wave is not a good approximation. Another source is

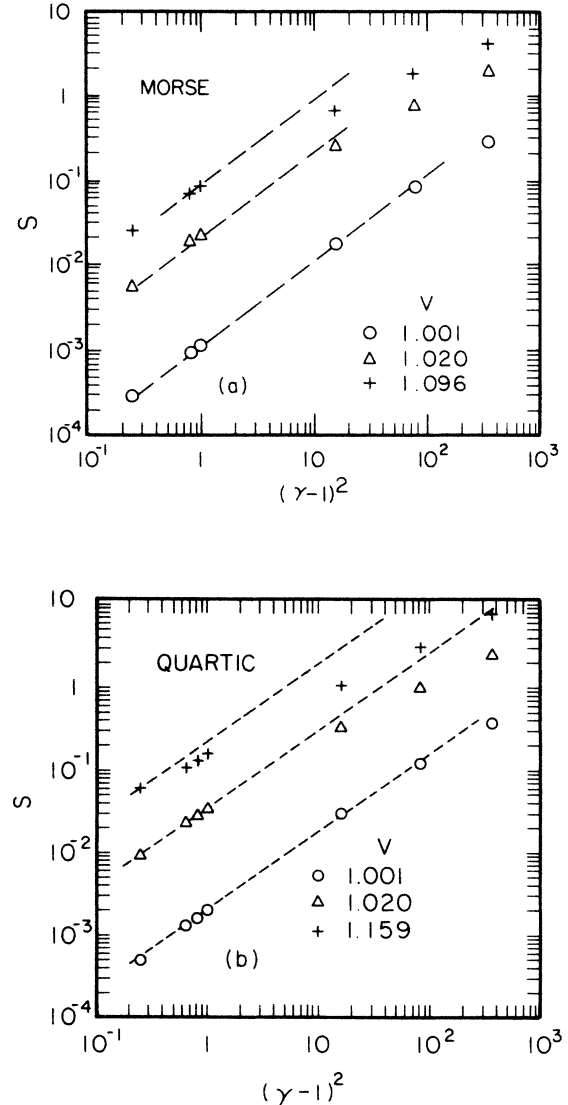


FIG. 2.  $S = 1/T_s - 1$  vs  $(\gamma - 1)^2$  dependence for three different incident energies. (a) Morse potential chain; ( $a = 7, p = 0.010204$ ),  $v = 1.001$ ,  $\circ: E_i = 0.141 \times 10^{-5}$ ;  $v = 1.020$ ,  $\triangle: E_i = 0.127 \times 10^{-3}$ ;  $v = 1.096$ ,  $+: E_i = 0.151 \times 10^{-2}$ . (b) Quartic potential chain ( $G = B = 1$ ),  $v = 1.001$ ,  $\circ: E_i = 0.518 \times 10^{-1}$ ;  $v = 1.020$ ,  $\triangle: E_i = 0.243$ ;  $v = 1.159$ ,  $+: E_i = 1.216$ . Dashed lines indicate the equivalent linear-plane-wave results for a convenient choice of the  $k$  parameter.

nonlinear effects—for narrow (high-energy) solitons, the nonlinearity becomes important. Hence, the linear approximation of the scattering process breaks down. This is discussed in detail in Sec. III B.

In Fig. 4 we plot the dependence of  $S$  on the incident soliton energy and the mass ratio for the envelope soliton, where only small-amplitude initial conditions are available. Here the linear wave-packet approximation describes even better the envelope soliton scattering from an impurity.

In Fig. 5 we plot the transmission coefficient  $T$  for the total energy versus  $\ln(\gamma)$  for three envelope initial conditions with a different wave vector  $k$  and a kink initial condition. In order to have comparable results, we take care to have the same incident energy for each soliton. From this plot it becomes clear that kink soliton is more robust against the impurity scattering. On the other

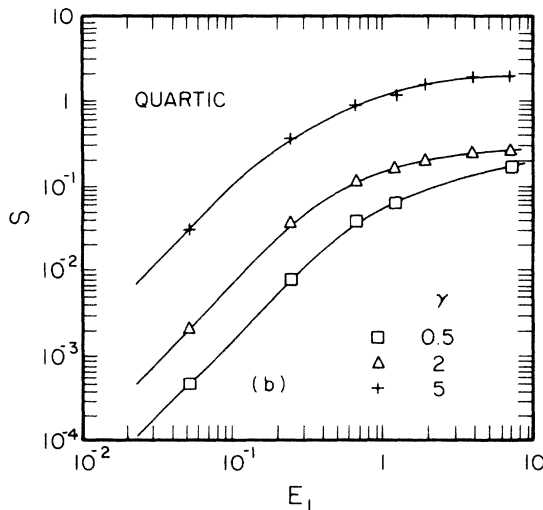
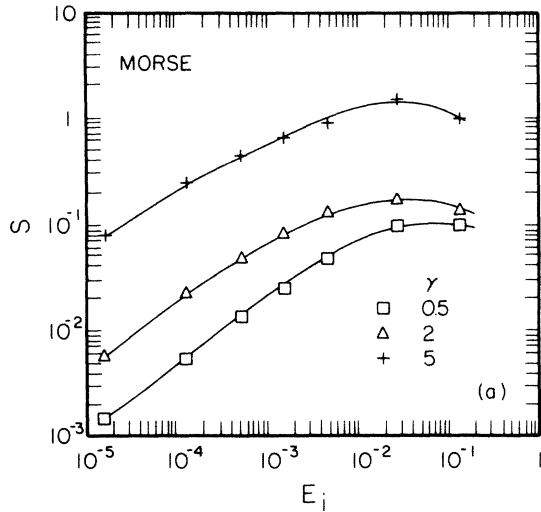


FIG. 3. Dependence of  $S=1/T-1$  on the incident soliton energy  $E_i$  for three different impurity masses. (a) Morse potential ( $a=7, p=0.010204$ ). (b) Quartic potential ( $G=B=1$ ).

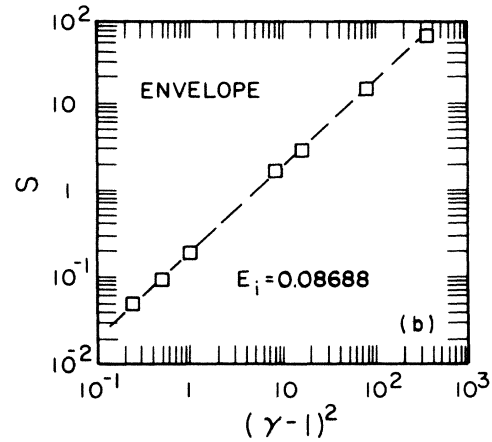
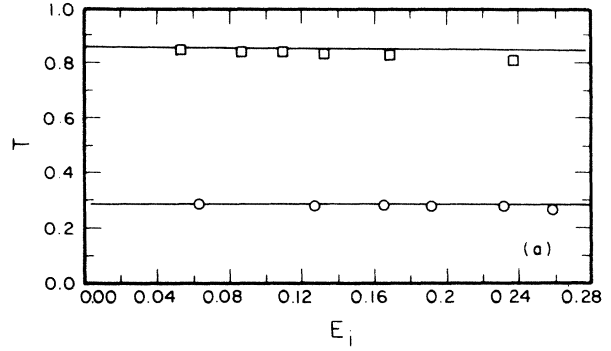


FIG. 4. (a) Total transmission coefficient  $T$  vs incident soliton energy  $E_i$  for envelope soliton.  $\square:k=0.8, \gamma=2$ ;  $\circ:k=2, \gamma=2$ . Solid lines indicate constant  $T$  of the linear-plane-wave transmission coefficient with wave vector  $k=K_\gamma$ . (b)  $S=1/T-1$  versus  $(\gamma-1)^2$  for envelope solitons in quartic potential. Dashed line indicates the equivalent linear-plane-wave results for a convenient choice of parameters.

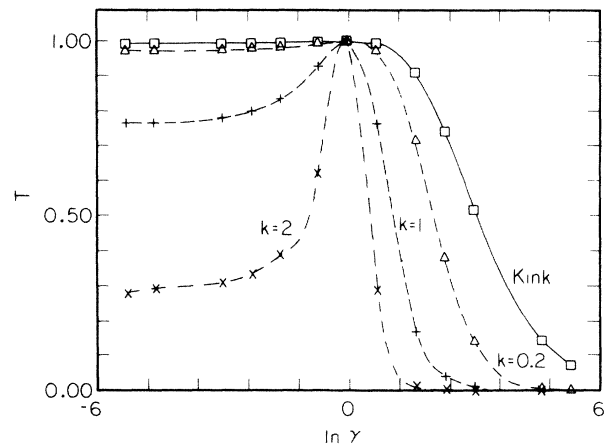


FIG. 5. Comparison of the transmission coefficient vs the impurity mass for one kink and three envelope incident solitons with different carrier wave vectors but comparable energies ( $E_i \approx 0.104$ ) in a quartic potential chain ( $G=B=1$ ).

hand, for envelope solitons, as the number of oscillations in the carrier wave increases (when  $k$  increases), the more the transmitted soliton loses energy. For small wave vector solitons (including kink), almost all the soliton energy is transmitted when  $\gamma \leq 1$ .

### B. Effects of strong nonlinearity

For a linear plane wave, the wave vector  $k$  is independent of the amplitude. Therefore, the transmission coefficient  $T_{LWP}$  is independent of the amplitude or the energy. On the other hand, for kink soliton, the amplitude, and consequently the energy  $E$ , are functions of  $K_s$ . Thus  $T_s$  depends on the amplitude  $A_m$  explicitly. When  $A_m$  becomes large, a full treatment of nonlinear effects is very difficult. Even Fourier transforming may have problems for narrow solitons due to discreteness effects. However, we treat that numerically by simulating linear scattering with initial wave packets having exactly the same shape with the corresponding soliton. Thus computing the transmission coefficient for the nonlinear chain on one hand, and for the equivalent harmonic chain on the other, we extract the effect of the nonlinearity. The results are shown in Fig. 6 for  $\gamma=2$  and  $\gamma=10$  for the Morse potential. We see that, for small energy,  $T_s \approx T_{LWP}$  is a good approximation, but solitons transmit much more in the higher energy regime. In other words, solitons are more robust. However, if we consider only the first soliton transmission coefficient  $T_1$ , the increased value of the nonlinear curve for high incident energies is less spectacular. This means that the high-energy incident soliton, in order to be better transmitted through the impurity scattering, is divided into more than one soliton. In the continuum limit (which is valid only for small-amplitude incident solitons), we can apply the inverse scattering method to predict the exact number of reflected and transmitted solitons. Therefore, asymptotic behavior can be predicted. However, a narrow soliton always means that the continuum limit breaks down.

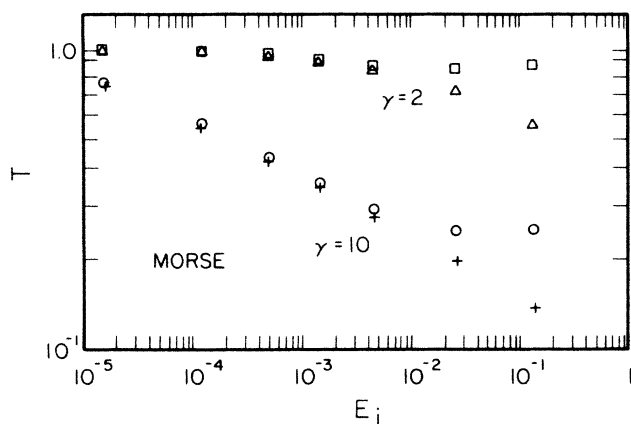


FIG. 6. Comparison of the total soliton transmission coefficient  $T_s$  of kink solitons ( $\square, \circ$ ) in a nonlinear Morse chain for two different impurity cases ( $\gamma=2, 10$ ) and that of same shape wave packet ( $\triangle, +$ ) in the equivalent harmonic chain with the same impurities. Solitons are more robust.

Hence, the scattering behavior in the strongly nonlinear regime is difficult to deal with.

### C. Two-impurity scattering and interference effects

It is well known that for linear plane waves more than one scatterer leads to interference effects. For solitons, we define interference in the sense that  $T \neq \prod_i T_i$ , where  $T_i$  is the total transmission coefficient of the  $i$ th scatterer. In Fig. 7 we show the dependence of the transmission coefficient  $T$  on the distance of two identical impurity scatterers for kink incident solitons in a Morse-type anharmonic chain. The interference effect can be seen clearly for small  $d$ . When  $d$  is larger than the extension of the soliton, i.e.,  $d > 2L$ ,  $T$  approaches  $T_1 T_2$ .

The envelope soliton case is especially interesting, since it follows the plane wave interference curve closely. In Fig. 8 we plot the total transmission coefficient  $T$  for two different envelope soliton energies in a quartic potential chain versus the impurity distance  $d$  and we compare with the plane wave result. When the distance  $d$  becomes comparable to the envelope width, then the interference effect saturates. Comparing results from Figs. 7 and 8, we conclude that the kink is much easier to transmit in disordered material than the envelope soliton, since there are always some local configurations which will effectively block the envelope soliton and make an important reflection.

It is well known that a localized mode is permitted above the cutoff frequency in a linear lattice with light impurity. The amplitude of this mode decreases exponentially with the distance from the impurity. In the present paper we have not studied the question of the excitation of the localized mode. However, this problem has been studied for small-amplitude kink solitons (in the

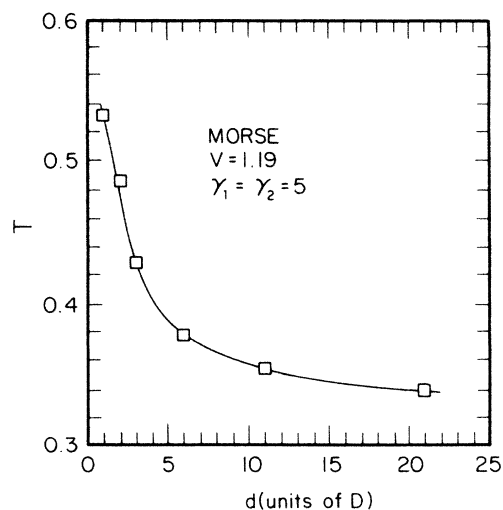


FIG. 7. Total transmission coefficient  $T$  for two-impurity scattering ( $M_1=M_2=5$ ) vs the impurities distance  $d$  for kink solitons ( $v=1.19$ ) in a Morse potential chain.  $T$  saturates around  $T_1 T_2$  which is the product of the independent scattering of the two impurities.

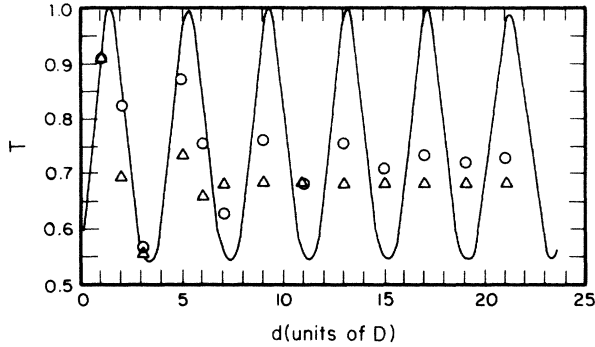


FIG. 8. Total transmission coefficient  $T$  for two-impurity scattering ( $M_1=M_2=2$ ) vs impurities distance  $d$  for envelope soliton ( $K=0.8$ ) in a quartic potential chain ( $G=B=1$ ). The solid line represents the linear-plane-wave scattering. Numerical points denote the envelope soliton scattering for two different incident energies ( $\circ: E_i=0.0869$ ,  $\triangle: E_i=0.2373$ ).  $T$  saturates around  $T_1 T_2$ .

continuum limit) both theoretically and numerically<sup>8,9</sup> as well as experimentally.<sup>4,5</sup> According to these works, a localized mode exists even in a nonlinear lattice, although some of the properties are modified by the nonlinearity: (i) the localized oscillation becomes anharmonic; and (ii) the frequency depends now on the amplitude. The localized mode can be excited more strongly through the interaction with a soliton having a width of the order of the impurity extension on the lattice ( $\sim D$ ). In this case the soliton impurity-interaction time is smaller than the semiperiod of the impurity eigenmode. If the characteristic frequency ( $v/L$ ) of the driving force (soliton) becomes comparable to the localized frequency, the interaction will occur resonantly. Envelope solitons cannot excite significantly the localized mode. Finally, kink solitons interacting with heavy mass impurities may excite a resonance mode with a relaxation time remarkably shorter.

#### IV. CONCLUSIONS

We have systematically studied the effects of nonlinearity on the simplest disordered system possible, that of one or two impurities in an otherwise perfect lattice.

Our numerical results show that the linear scattering approximation is valid for low energies, i.e., small-amplitude solitons. For high enough energies, the cohesiveness due to the nonlinearity becomes apparent and the linear scattering breaks down, and a new theory is needed. In general, our results showed that solitons are more robust than linear wave packets and that the kink soliton is more robust than envelope solitons.

For the two-impurities case, we have strong interfering effects which for some energies help the soliton to go through more easily than the less disordered case of one impurity.

We, therefore, predict that kink solitons can survive the disorder and propagate in the disordered medium better than a linear wave packet. Therefore, solitons must be excitations which live longer than linear wave packets in disordered media.

It is important to note that our results indicate a nonexponential decay of a soliton in a disordered nonlinear medium in contrast to what happens to a plane wave propagating in a linear disorder medium. In the latter, each scattering center takes away a fixed fraction of the wave independently of the amplitude, and this leads to exponential decay. In the nonlinear case, the scattered fraction of the soliton depends explicitly on the amplitude and hence, the decay law is complicated and specific.

It will be, of course, very interesting to study the effects of the nonlinearity on a disordered system having a finite amount of impurities. The behavior of the localization length with the strength of disorder in the presence of the nonlinearity might be different than the one without the nonlinearity. These studies will need a substantial amount of computer time to be completed. Finally, the behavior of the propagation of a soliton in a disordered chain with substrate will be also interesting to study.

#### ACKNOWLEDGMENTS

Ames Laboratory is operated for the United States Department of Energy by Iowa State University under Contract No. W-7405-Eng82.

#### APPENDIX A

From (2.5) the kink-type solution for the atomic displacement  $y(x, t)$  is<sup>2,3</sup>

$$y(x, t) = \pm 2(\text{sgn} h)(2h/q)^{1/2} \tan^{-1} \times \{ (1/w) \tanh[(x-vt)/L] \} \quad (\text{A1})$$

with

$$W = \left[ \frac{[4p^2 + 18(v^2 - c_0^2)q]^{1/2} \pm 2p}{[4p^2 + 18(v^2 - c_0^2)q]^{1/2} \mp 2p} \right]^{1/2} \quad (\text{A2})$$

and

$$L = 2[h/(v^2 - c_0^2)]^{1/2}. \quad (\text{A3})$$

For  $q=0$  (Boussinesq equation case) (A1) becomes

$$y(x, t) = A_m \tanh[(x-vt)/L] \quad (\text{A4})$$

with the total energy of the excitation given by:

$$E_t = \frac{4}{15} \frac{M}{D} K_s A_m^2 (4v^2 + c_0^2), \quad (\text{A5})$$

where

$$A_m = \text{sgn}(h) 2[h(v^2 - c_0^2)]^{1/2}/p \quad \text{and} \quad K_s = 1/L.$$

For  $p=0$  ( $M-Bq$  equation case) we have

$$y(x, t) = A_m \tan^{-1} \{ \exp[2(x-vt)/L] \} \quad (\text{A6})$$

with the total energy given by

$$E_t = \frac{1}{6} \frac{M}{D} K_s A_m^2 (2v^2 - c_0^2), \quad (\text{A7})$$

where  $A_m = \pm 2(h/q)^{1/2}$  and  $K_s = 2/L$ .

## APPENDIX B

The envelope-type soliton for the atomic displacement  $y(x, t)$  is<sup>2,3</sup>

$$y(x, t) = A_m \operatorname{sech}[(x - v_e t)/L_e] \cos[(x - v_0 t)/L_0] \quad (\text{B1})$$

with

$$A_m = 4\eta/K_0^{1/2}, \quad v_e = v_g - 2\alpha\mu, \quad L_e = 1/2\eta, \quad (\text{B2})$$

$$v_0 = [\omega - 2\alpha v_g + 2\mu(\alpha^2 - \eta^2)]/(k - 2\alpha),$$

$$L_0 = 1/(k - 2\alpha),$$

where  $\eta$  and  $\alpha$  are small arbitrary parameters and  $k$  takes values in the first Brillouin zone of the harmonic chain.

\*Permanent address: Ames Laboratory and Department of Physics, Iowa State University, Ames, IA 50011.

<sup>1</sup>E. Fermi, J. R. Pasta, and S. Ulam, Los Alamos Scientific Laboratory Report No. LA-1940, 1955 (unpublished).

<sup>2</sup>St. Pnevmatikos, C. R. Acad. Sci. Paris **296**, 1031 (1983); see also *Singularities and Dynamical Systems*, edited by St. Pnevmatikos, (North-Holland, Amsterdam, 1985), Vol. 103, p. 397.

<sup>3</sup>N. Flytzanis, St. Pnevmatikos, and M. Remoissenet, J. Phys. C **18**, 4603 (1985).

<sup>4</sup>S. Watanabe and M. Toda, J. Phys. Soc. Jpn. **50**, 3443 (1981).

<sup>5</sup>T. Efthimiopoulos, N. Flytzanis, and St. Pnevmatikos (unpublished).

<sup>6</sup>W. M. Visscher, in *Methods in Computational Physics* (Academic, New York, 1976), Vol. 15, p. 371, and references therein.

<sup>7</sup>M. Toda, Phys. Scr. **20**, 424 (1979).

<sup>8</sup>A. Nakamura, Prog. Theor. Phys. **59**, 1447 (1978); S. Watanabe and M. Toda, J. Phys. Soc. Jpn. **50**, 3436, (1981); F. Yoshida and T. Sakuma, Prog. Theor. Phys. **67**, 1379 (1982); **68**, 29

(1982); T. Klinker and W. Lauterborn, Physica **8D**, 249 (1983).

<sup>9</sup>F. Yoshida and T. Sakuma, Prog. Theor. Phys. **60**, 338 (1978).

<sup>10</sup>N. Yajima, Prog. Theor. Phys. **58**, 114 (1977); F. Yoshida and T. Sakuma, J. Phys. Soc. Jpn. **42**, 1412 (1977).

<sup>11</sup>N. Flytzanis, St. Pnevmatikos, and M. Peyrard Physica **26D**, 311 (1987); see also M. Peyrard, St. Pnevmatikos, and N. Flytzanis, Physica **19D**, 268 (1986).

<sup>12</sup>E. N. Economou, *Green's Functions in Quantum Physics* (Springer, Berlin, 1983).

<sup>13</sup>M. A. Collins, Chem. Phys. Lett. **77**, 342 (1981); in, *Advances in Chemical Physics*, edited by I. Prigogine and S. A. Rice, (Wiley, New York, 1983), Vol. 53, p. 225.

<sup>14</sup>St. Pnevmatikos, N. Flytzanis, and M. Remoissenet, Phys. Rev. B **33**, 2308 (1986).

<sup>15</sup>E. N. Economou and C. M. Soukoulis, Phys. Rev. Lett. **46**, 618 (1981); **47**, 973 (1981); Phys. Rev. B **24**, 5698 (1981); Solid State Commun. **37**, 409 (1981).

<sup>16</sup>F. Delyon, Y. E. Levy, and B. Souillard, Phys. Rev. Lett. **57**, 2010 (1987).